PREVENTION OF MUSCLE DISUSE ATROPHY BY MG132 PROTEASOME INHIBITOR

CECILE JAMART, MS, JEAN-MARC RAYMACKERS, MD, PhD, GANG LI AN, MS, LOUISE DELDICQUE, PhD, and MARC FRANCAUX, PhD

Research Group in Muscle and Exercise Physiology, Institute of Neuroscience, Université Catholique de Louvain, Place Pierre de Coubertin 1, Louvain-la-Neuve B-1348, Belgium

ABSTRACT: *Introduction*: Our goal was to determine whether in vivo administration of the proteasome inhibitor MG132 can prevent muscle atrophy caused by hindlimb unloading (HU). *Methods*: Twenty-seven NMRI mice were assigned to a weight-bearing control, a 6-day HU, or a HU+MG132 (1 mg/kg/48 h) treatment group. *Results*: Gastrocnemius wasting was significantly less in HU+MG132 mice ($-6.7 \pm 2.0\%$) compared with HU animals ($-12.6 \pm 1.1\%$, $P = 0.011$). HU was also associated with an increased expression of MuRF-1 ($P = 0.006$), MAFbx ($P = 0.001$), and USP28 ($P = 0.027$) mRNA, whereas Nedd4, E3α, USP19, and UBP45 mRNA did not change significantly. Increases in MuRF-1, MAFbx, and USP28 mRNA were largely repressed after MG132 administration. β5 proteasome activity tended to increase in HU ($+16.7 \pm 6.1\%$, $P = 0.086$). Neither β1 and β2 proteasome activities nor ubiquitin-conjugated proteins were changed by HU. *Conclusions*: Our results indicate that in vivo administration of MG132 partially prevents muscle atrophy associated with disuse and highlight an unexpected regulation of MG132 proteasome inhibitor on ubiquitin-ligases.

Muscle unloading is characterized by a prolonged period of inactivity through which muscle contractile activity and tension are markedly decreased. Settings of muscle disuse, such as bed rest, trauma, or a microgravity environment, result in rapid skeletal muscle atrophy due to an imbalance between protein synthesis and degradation. The functional consequence of muscle atrophy is a general muscle weakness that can impair daily motion activities and, in severe cases, have survival implications. Therefore, a number of studies dealing with strategies to prevent skeletal muscle atrophy due to

inactivity have been undertaken in recent years. Among them, hindlimb-unloading (HU) experiments have shown that the negative protein balance is at least due partly to enhanced proteolysis.[1,2] Three major proteolytic pathways have been described in the skeletal muscle cell: the Ca^{2+}-dependent pathway; the lysosomal pathway; and the ubiquitin–proteasome pathway (UPP). There is evidence that the latter is responsible for the degradation of the bulk of the proteins and that this pathway is activated during HU.[1,3,4] Therefore, the use of therapeutic agents that repress the increase in UPP activity with unloading may be of interest.

Briefly, the UPP works in two steps. The first step is characterized by the covalent linkage of a polyubiquitin chain to the protein target. This linkage is allowed by the sequential action of three enzymes: E1 or ubiquitin-activating enzymes; E2 or ubiquitin-carrying enzymes; and E3, also called ubiquitin-ligases. There are several hundred E3s, and they ensure the specificity of the UPP by targeting specific proteins. Among them, muscle RING finger-1 (MuRF-1) and atrogin-1/muscle atrophy F-box (MAFbx), two muscle-specific ligases, are known to be increased in numerous models of atrophy.[5] Neural precursor cell-expressed developmentally downregulated 4 (Nedd4) and E3α are other ligases that have been shown to increase in HU and a unilateral hindlimb immobilization model of atrophy, respectively.[6,7] The second step of UPP implies degradation of the ubiquitinated protein by the 26S proteasome. The central part of the 26S proteasome is the catalytic core—called 20S—inside which the proteolytic sites are localized. Three main catalytic activities have been described: caspase-like, trypsin-like, and chymotrypsin-like activities, which are associated with the β1, β2, and β5 subunits, respectively.[8] More recently, attention has been paid to another enzyme family implicated in the UPP: de-ubiquitinating enzymes (DUBs). Although their role in skeletal muscle atrophy is not yet clear, some DUBs have been reported to increase in atrophy models.[6,9]

Proteasome inhibitors are among the drugs that target the UPP.[8] They can be divided into several classes. In research, the most widely used class of inhibitors are peptide aldehydes,[8] from which the most potent inhibitor is MG132. Two studies

have shown that, in rats submitted to denervation or cecal ligation and puncture (CLP), ex vivo MG132 incubation of muscles repressed the accelerated proteolysis by >50%.[10,11] In other in vivo studies, local injection of MG132 in the gastrocnemius muscle of *mdx* mice—the murine model for Duchenne muscular dystrophy—rescued muscle structure,[12] and intraperitoneal administration of MG132 at 3 hours after CLP surgery prolonged mouse survival.[13] More recently, Supinski et al. reported that MG132 was able to rescue endotoxin-induced proteolysis in the diaphragm muscle of rats.[14] Until now, few studies have been done on the effects of proteasome inhibitor administration in unloading atrophy models[15,16] and, to the best of our knowledge, no study has been done with HU. Therefore, the purpose of our study was to evaluate the potential beneficial effects of MG132 administration in vivo in the HU atrophy model and to assess the signaling pathways implicated.

METHODS

Animal Care. Twenty-seven male NMRI mice (11–14 weeks old) were obtained from the animal facilities of the Université Catholique de Louvain. Animals were housed at 22°C on a 12-h dark–light cycle with ad libitum access to food and water. All procedures were approved by the local committee for ethical practices in animal experiments, and the housing conditions were as specified by the Belgian Law of November 14, 1993, on the protection of laboratory animals (Agreement No. LA 1220548). One week after arrival, mice were placed individually in a large cage and left for 2 days of acclimation during which food and water were accessible on the ground only. Water was kept in a small dish and replenished every day.

Hindlimb Suspension. Mice were randomly assigned to either a control group (CTRL, $n = 9$), hindlimb unloaded group (HU, $n = 9$), or hindlimb unloaded plus MG132 treatment group (HU+MG132, $n = 9$). On the first day of the experiment the mice were weighed. They were then injected with vehicle (CTRL and HU) or MG132 (HU+MG132). HU and HU+MG132 animals were suspended. A piece of orthopedic tape was wrapped around the tail in order to fix an unfolded paper clip (8-shaped). The paper clip was attached to a swivel, which allowed 360° of motion on the forelimbs. The swivel was fastened to the top of the cage by nylon rope. Care was taken so that mice were not able to use their hindlimbs on any side of the cage, and they could not hang on the grid. Suspension duration was 6 days.

MG132 Administration. HU+MG132 animals were injected intraperitoneally every other day with MG132 solution (1 mg/kg/48 h; Merck, Darmstadt, Germany). CTRL and HU groups were injected with vehicle (2.1% dimethylsulfoxide in saline solution).

Anesthesia. At the end of the suspension period, the mice were anesthetized with a mixture of ketamine (200 mg/kg) and xylazine (20 mg/kg) while they were still suspended. Animals were detached and weighed. Right and left gastrocnemius muscles were excised, weighed, and frozen in liquid nitrogen. After dissection, mice were terminally anesthetized with an additional dose of ketamine–xylazine. Muscles were kept at −80°C before further analysis.

Time-Course of 20S Proteasome Inhibition by MG132. Twenty-four male NMRI mice (12 weeks old) were obtained and housed as described previously. They were injected intraperitoneally with 1 mg/kg MG132 ($n = 21$) or vehicle (CTRL, $n = 3$). MG132-treated animals were killed after 30 min and 1, 2, 4, 8, 24, and 48 h ($n = 3$ at each time-point). Animals from the CTRL group were killed 1.5 h after vehicle injection. Gastrocnemius muscles were excised, frozen in liquid nitrogen, and kept at −80°C before further analysis. Proteasome activity assay was done using the technique as described in what follows.

Cell Culture. C2C12 cells were purchased from the ATCC (Manassas, Virginia) and incubated at 37°C in a humidified atmosphere of 5% CO_2. Myoblasts were grown in Dulbecco modified Eagle medium (DMEM) containing 10% fetal bovine serum (FBS), 100 μM non-essential amino acids, 200 U/ml penicillin, 200 μg/ml streptomycin, and 4.5 g/L glucose, until 70% confluence, and then differentiated for 120 h in a medium in which FBS was replaced by 1% horse serum. MG132 or vehicle was added to culture medium at a final concentration of 10 μM for 20 h. Cells were harvested using the method described by Deldicque et al.[17]

Protein Extraction. Whole muscles were crushed in a mortar in liquid nitrogen and homogenized in ice-cold buffer containing 50 mM Tris-HCl (pH 8.0), 1 mM ethylene-glycol tetraacetic acid (EGTA), 1 mM ethylene-diamine tetraacetic acid (EDTA), a protease inhibitor cocktail (Roche Applied Science, Vilvoorde, Belgium), and 10% glycerol. The cytosolic fraction was obtained from the centrifugation of homogenates twice at $1500g$ for 10 min and once at $10,000g$ for 15 min, at 4°C. Supernatants were conserved at −80°C. Myofibrillar fractions were extracted from the pellet of the first centrifugation. Pellets were washed three times in ice-cold buffer plus 1% Triton X-100,

resuspended in a buffer containing 50 mM Tris-HCl (pH 7.5), 8 M urea, and a protease inhibitor cocktail, and stored at $-80°C$. Protein content of each fraction was determined in duplicate using a DC protein assay kit (Bio-Rad, Nazareth Eke, Belgium) with bovine serum albumin as a standard.

Sodium Dodecylsulfate–Polyacrylamide Gel Electrophoresis and Immunoblotting. Twenty-five to 40 μg of proteins were combined with Laemmli sample buffer. Cytosolic fractions were separated by sodium dodecylsulfate–polyacrylamide gel electrophoresis (SDS-PAGE) for 1 h at a constant intensity of 40 mA. Myofibrillar fractions were run overnight at 40 V using 4–15% gradient gels from Bio-Rad. Proteins were transferred on polyvinylidene fluoride (PVDF) membranes at 80 V for 2–4 h. Membranes were blocked 1 h in Tris-buffered saline plus 0.1% Tween 20 (TBST) and 5% nonfat dry milk, then incubated overnight at 4°C with one of the following primary antibodies: phospho-Akt(Ser473), phospho-Akt(Thr308), phospho-FoxO1(Thr24) / FoxO3a(Thr32), IκBα, and ubiquitin (all from Cell Signaling Technology, Leiden, The Netherlands); and proteasome 20S $\alpha + \beta$ and glyceraldehyde 3-phosphate dehydrogenase (GAPDH) (both from Abcam, Cambridge, UK). Membranes were washed three times with TBST and incubated for 1 h at room temperature with a secondary antibody conjugated to horseradish peroxidase. Three washings were made again before detection by chemiluminescence (Amersham ECL-Plus Western Blotting Kit; GE Healthcare, Diegem, Belgium). Films were scanned on an ImageScanner using LabScan software, and bands were quantified with image analysis software (Image Master 1D; Amersham–GE Healthcare). GAPDH was used to ensure equal loading for the cytosolic fraction. Ensuring proper loading of myofibrillar proteins was done by staining membranes with Coomassie blue.

20S Proteasome Activity Assay. β1, β2, and β5 proteasomal activities were assessed on a 96-well black plate (Greiner Bio One; Wemmel, Belgium) by the release of 7-amino-4-methylcoumarin (AMC) using specific substrates from Merck for each type of activity [Z–Leu–Leu–Glu–aminomethylcoumarin (Z-LLG-AMC), Z–Ala–Arg–Arg–aminomethylcoumarin (Z-ARR-AMC), and Suc–Leu–Leu–Val–Tyr–aminomethylcoumarin (Suc-LLVY-AMC), respectively]. Ten micrograms of cytosolic proteins, 200 μl of buffer [Tris-HCl 50 mM (pH 8), MgCl$_2$ 5 mM, and dithiothreitol (DTT) 1 mM], and 100 μM fluorescent-specific substrate were put in each well. Each sample was realized in quadruplicate for each activity, one of them being incubated with 50 μM MG132 to assess specificity of the activity. Fluorescence intensity was measured at 37°C during 30 min on a fluorometer (Fluoroskan Ascent FL; Thermo Scientific, Zellik, Belgium). One measurement was done every 2 min at excitation and emission wavelengths of 370 nm and 460 nm, respectively. Activities were calculated as the slope of the accumulation of fluorescence as a function of time and were expressed relative to an internal control sample that had been put on each plate.

RNA Extraction and Quantitative Real-Time PCR. Tissue samples were homogenized with a pestle in 1 ml of Trizol reagent (Invitrogen, Vilvoorde, Belgium), and RNA was isolated according to the manufacturer's instructions. RNA quality and quantity were assessed by 1.5% agarose gel electrophoresis and Nanodrop spectrophotometry. Reverse transcription (RT) was performed on MyIQ2 thermocycler (Bio-Rad). Firstly, 1.5 μg of RNA was added with 1 μl of oligo-dT$_{12-18}$ primers, 1 μl DNTPs, and RNase-free water for a final volume of 12 μl that was run for 5 min at 65°C. For the second step (2 min, 42°C), 4 μl of 5× first-strand buffer, 2 μl of 0.1 M DTT, and 1 μl RNase-OUT were added to the samples. Finally, 1 μl of Superscript II was added, and the final RT product was obtained after a run of 50 min at 42°C and 15 min at 72°C. Primers used for quantitative PCR are reported in Table 1. Cyclophilin (Cphn) was used as a reference gene. Experiments were performed on a MyIQ2 thermocycler, under the following conditions: 3 min at 95°C, followed by 35 cycles of 30 s at 95°C, 30 s at 60°C, and 30 s at 72°C. Genes were analyzed in triplicate for each sample in a 25-μl reaction volume containing 12.5 μl of IQ Sybr-Green SuperMix (Bio-Rad), 0.5 μl of each primer (100 nM final), and 12 μl of cDNA with the appropriate dilution. Melting curves were systematically assessed for quality control. Data were normalized to Cphn, which remained unchanged.

Statistical Analysis. Values are presented as mean $\pm$ SEM. A one-way analysis of variance (ANOVA), followed by a Student–Newman–Keuls post hoc test, was used for statistical analysis. Statistical significance was set at $P < 0.05$.

RESULTS

Body and Muscle Weight. After 6 days of suspension, body weight was diminished by 4.9 $\pm$ 1.5% in the HU group ($P = 0.028$), which was not reversed by MG132 treatment (Table 2). The gastrocnemius muscle weight was 12.6 $\pm$ 1.1% lower in HU compared with CTRL animals ($P < 0.001$). After MG132 administration, gastrocnemius muscle was significantly heavier than in the HU group ($P = 0.011$) as muscle weight was 6.7 $\pm$ 2.0% lower in HU+MG132 compared with CTRL ($P = 0.005$). The ratio of gastrocnemius/body weight of the

HU animals was $11.0 \pm 1.2\%$ lower than that of the CTRL group ($P < 0.001$). In MG132-treated animals, the ratio was only $5.7 \pm 1.6\%$ lower than that of the CTRL group ($P = 0.009$), and it was significantly greater than in the HU group ($P = 0.012$) (Table 2).

Components of the Ubiquitin–Proteasome Pathway. MuRF-1 and MAFbx mRNA expression levels were higher in HU animals than in CTRL animals by 2.7 ± 0.5-fold ($P = 0.006$) and 2.2 ± 0.2-fold ($P = 0.001$), respectively (Fig. 1A). Nedd4 mRNA was increased by 1.8 ± 0.3-fold, but this change did not reach statistical significance ($P = 0.144$). The level of E3α mRNA was not different in the three conditions (Fig. 1A). When MG132 was administered to HU animals, the increase in MuRF-1 mRNA was almost completely blunted (HU+MG132 vs. HU: $P = 0.005$) and was reduced by about two-thirds for MAFbx (HU+MG132 vs. HU: $P = 0.010$). Nedd4 mRNA expression was not affected significantly by MG132. The amount of ubiquitin-conjugated proteins (UbCPs) was unaffected either by HU or by MG132 in vivo even though C2C12 cell incubation with 10 μM MG132 for 20 h increased UbCPs by 12.6 ± 2.5-fold ($P = 0.010$, Fig. 1B). USP28 mRNA was 1.7 ± 0.2-fold higher ($P = 0.027$) in HU animals. The increase was reversed by 90.9% with MG132 (HU+MG132 vs. HU: $P = 0.018$) (Fig. 1C).

Two other de-ubiquitinating enzymes (USP19 and UBP45) were unaffected, regardless of the condition studied. HU tended to increase proteasome $\beta5$ activity ($+16.7 \pm 6.1\%$; $P = 0.086$), whereas $\beta1$ and $\beta2$ activities were unchanged. MG132 administration did not change proteasome activity in vivo, whereas incubation of C2C12 cells with 10 μM MG132 for 20 h reduced $\beta5$ activity by 94.1% ($P < 0.001$; Fig. 1D). The protein level of proteasome 20S $\alpha + \beta$ subunits remained unaffected by any condition (Fig. 1E).

Regulation of Ligase mRNA Expression. Because of the unexpected results for ligases, we measured markers of activation of the main transcription factors currently known to regulate mRNA ligase expression: nuclear factor–kappa light-chain enhancer of activated B cells (NF-κB) and forkhead box O (FoxO).[18] Under basal conditions, NF-κB family members are kept in the cytosol by the NF-κB inhibitor protein nuclear factor of kappa light polypeptide gene enhancer in B cells inhibitor alpha (IκBα). Under atrophy signal, IκBα becomes phosphorylated, which marks it for ubiquitination and subsequent proteasomal degradation. Therefore, MG132 could possibly regulate ligase mRNA expression by preventing IκBα degradation. Under the present conditions, cytosolic IκBα protein expression remained unaffected

Table 2. Body and gastrocnemius weight.

Parameter	CTRL ($n = 9$)	HU ($n = 9$)	HU+MG132 ($n = 9$)
Initial body weight (g)	41.4 ± 0.7	40.9 ± 1.0	41.1 ± 0.8
Final body weight (g)	41.2 ± 1.0	38.9 ± 1.2	39.0 ± 0.8
Body weight change (%)	-0.62 ± 1.23	-4.94 ± 1.50*	-4.97 ± 1.17
Gastrocnemius weight (mg)	193.8 ± 2.8	169.3 ± 2.1‡	180.8 ± 4.0†,§
Gastrocnemius weight/body weight ratio (mg/g)	4.67 ± 0.07	4.15 ± 0.06‡	4.40 ± 0.08†,§

Weight of gastrocnemius was measured in left and right muscles. Values expressed as mean ± SEM. CTRL, controls; HU, hindlimb unloading.
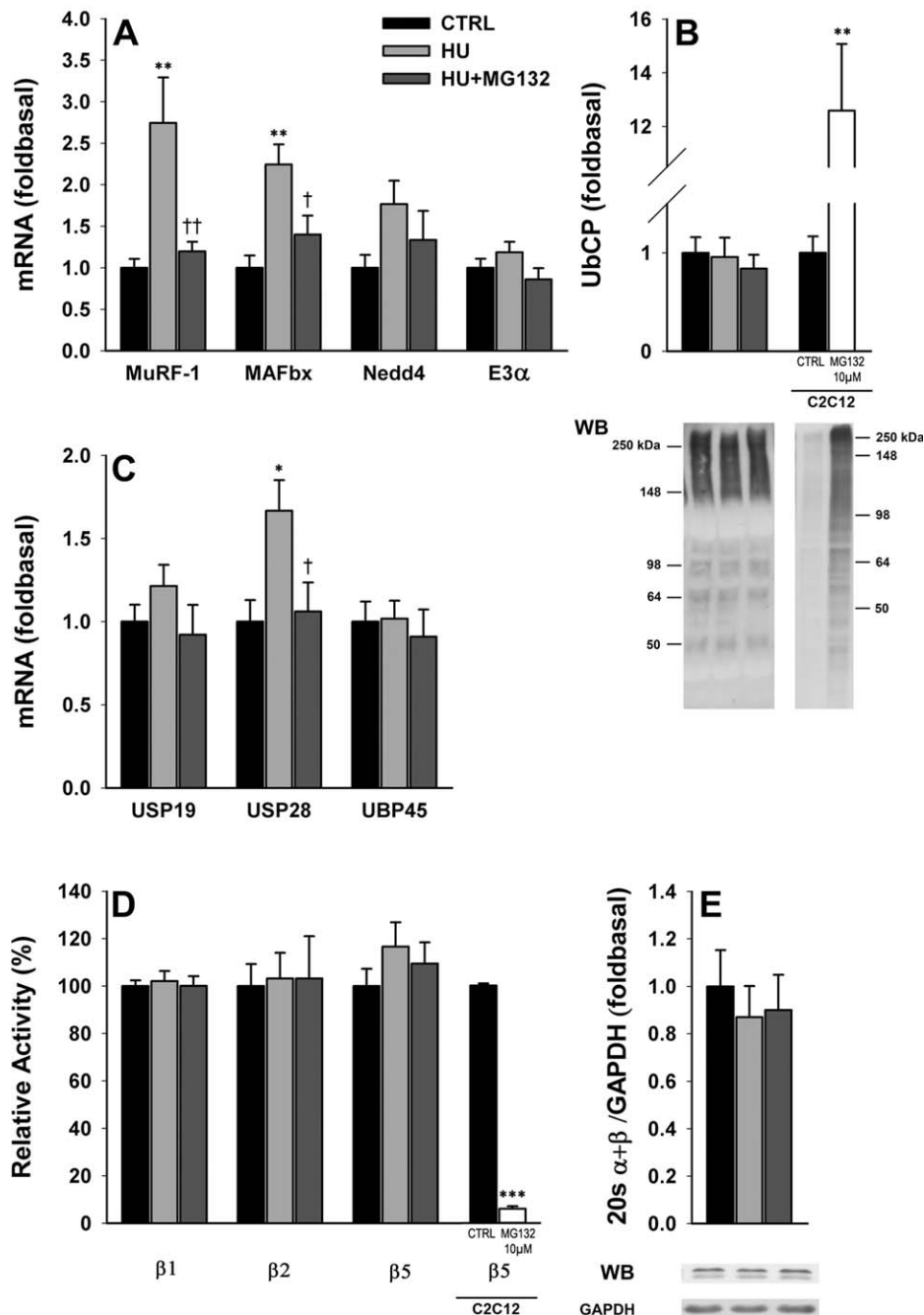*$P < 0.05$.
†$P < 0.01$.
‡$P < 0.001$ vs. CTRL.
§$P < 0.05$ vs. HU.

FIGURE 1. Effects of 6 days of HU and MG132 treatment on expression of gastrocnemius mRNA ligases **(A)**, ubiquitin-conjugated protein (UbCP) expression; a positive control obtained in myogenic C2C12 cells after 10 μM MG132 administration is provided **(B)**, DUB mRNA expression **(C)**, proteasome activity; a positive control obtained in myogenic C2C12 cells after 10 μM MG132 administration is provided **(D)** and proteasome 20S $\alpha + \beta$ protein expression **(E)**. Representative Western blots are shown below their respective bars. Values are expressed as mean $\pm$ SEM. $^*P < 0.05$, $^{**}P < 0.01$, and $^{***}P < 0.001$ vs. CTRL; $^\dagger P < 0.05$ vs. HU.

either by HU or by HU+MG132 treatment (Fig. 2A). Another pathway known to regulate muscle ligase mRNA expression is the Akt/FoxOs pathway. Disuse signaling results in inactivation of Akt and thereby dephosphorylation of FoxOs, which translocate to the nucleus and activate transcription of target genes. We measured phosphorylation states of Akt, FoxO1, and FoxO3a, but they remained unaffected under the present conditions (Fig. 2B).

Time-Course of 20S Proteasome Inhibition by MG132. The pharmacodynamic profile of MG132 was evaluated by measuring β5 activity in gastrocnemius of NMRI mice injected intraperitoneally with 1 mg/kg MG132. The time-course of 20S proteasome inhibition by MG132 is shown in Figure 3. Proteasome β5 activity of gastrocnemius decreased between 2 and 8 h after injection to reach 12% inhibition compared with control muscles from
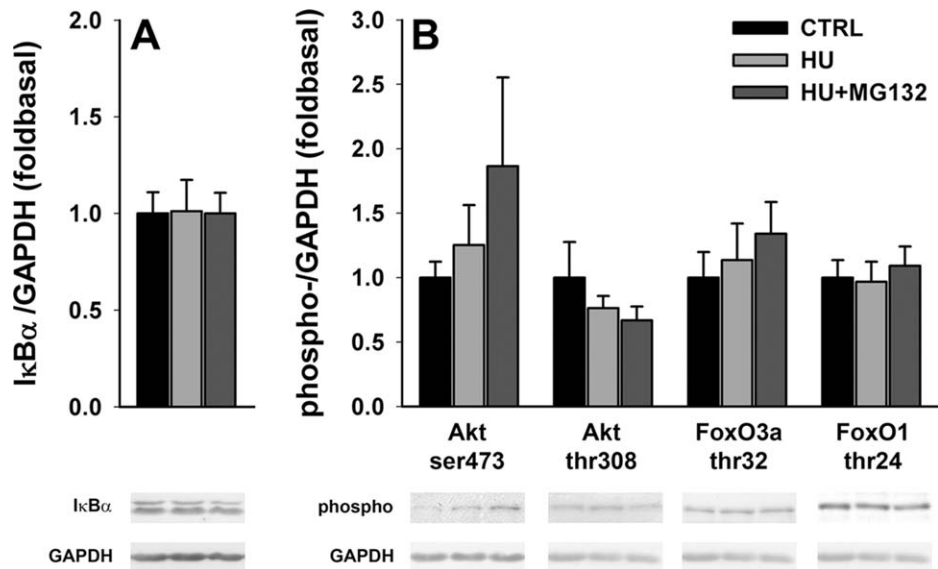
FIGURE 2. Effects of 6 days of HU and MG132 treatment on markers of pathways known to regulate expression of mRNA muscle ligases. Levels of IκBα **(A)** and phosphorylated forms of Akt, FoxO1, and FoxO3a **(B)** are normalized to levels of GAPDH and compared with their expression in control muscles. Representative Western blots are shown below their respective bars. Values are expressed as mean ± SEM.

vehicle-injected mice. Then, proteasome β5 activity re-increased progressively over time, but it was still slightly lower 48 h after injection (−8%). This was in accordance with the results obtained in the HU+MG132-treated group.

DISCUSSION

The gastrocnemius muscle atrophy that we observed after a 6-day HU period in mice (12.6 ± 1.1%) was similar to that observed in previous studies carried out on the same model.[5,19] We showed that in vivo administration of the proteasome inhibitor MG132 was effective for rescuing muscle mass in a disuse atrophy model. The dose of drug administered was 1 mg/kg, which is similar to the amount used in other in vivo animal studies.[13,14] Bortezomib, another proteasome inhibitor, has been administered twice per week in patients with refractory hematologic malignancies.[20] To investigate a clinically relevant administration schedule, MG132 was administrated every 2 days in this study. This regimen reduced gastrocnemius atrophy by about 50%, but it did not reverse body weight loss, suggesting a muscle-specific action of MG132. Holecek et al.[21] reported that MG132 administered in vivo inhibited β5 activity of proteasome in skeletal muscle, but not in other organs. In our study, we showed that MG132 affects two other components of the ubiquitin–proteasome pathway, namely the muscle-specific ubiquitin-ligases MuRF-1 and MAFbx (Fig. 1A) and USP28 de-ubiquitinase (Fig. 1C).

Muscle-specific ligase MuRF-1 and MAFbx mRNAs have been reported to be upregulated in various muscle atrophy models and seem to be part of a common program activated in all atrophy models.[5] This is not the case for Nedd4, which has been shown to increase during atrophy due to reduced muscle tension but not in cachexia-related atrophy.[22] In accordance with the literature,[5] we found that HU induced a clear increase in mRNA expression of MuRF-1 and MAFbx. The increase in Nedd4 mRNA expression following HU did not reach statistical threshold under our conditions. Even as E3α mRNA expression was reported to increase in unilateral hindlimb immobilization,[6] it did not change in our conditions.

De-ubiquitinase function in skeletal muscle atrophy is much less clear than that for ubiquitin-ligases. It seems that DUBs can behave as either pro- or anti-atrophic components of the UPP pathway. They can spare proteasome substrates from degradation, yet they can recycle ubiquitin after substrate degradation or process the translational product of the polyubiquitin gene to its mature form.[23] We observed a significant increase in
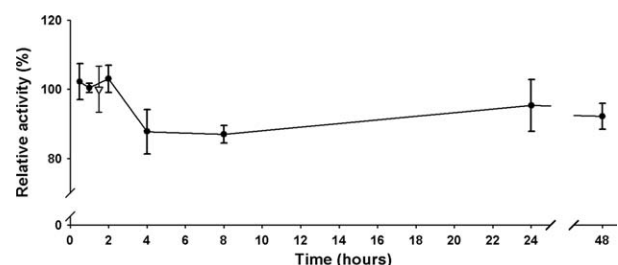
FIGURE 3. Time-course of proteasome β5 activity in gastrocnemius muscle of NMRI mice after an intraperitoneal injection of 1 mg/kg MG132 (filled circles) or after injection of the vehicle (open triangle). Values are expressed as mean ± SEM ($n = 3$ at each time-point).

USP28 mRNA under atrophy due to HU. The same trend was observed recently by Baptista et al. in a model of unilateral hindlimb immobilization.[6] The fact that an increase in USP28 was repressed by MG132 administration suggests that ligases like MuRF-1 and MAFbx share a common pathway of regulation with de-ubiquitinases like USP28. Even as USP19 and UBP45 mRNA were reported to increase in various atrophy models,[6,9] they did not change in our HU model.

The increase in MuRF-1, MAFbx, and USP28 mRNA was largely repressed after MG132 administration. Two major pathways have been implicated in the regulation of muscle-specific ligase mRNA expression during disuse atrophy: the NF-κB pathway and the IGF-1/PI3K/Akt pathway.[24] Translocation of NF-κB factors into the nucleus is permitted when proteasomal IκBα degradation occurs. Therefore, MG132 can prevent NF-κB activation by inhibiting IκBα degradation. Under our conditions, IκBα was unchanged after 6 days of HU. Nevertheless, we cannot rule out implications of this pathway in the repression of ligase mRNA, because IκBα may have been degraded at the onset of the unloading period and returned to basal levels after 6 days, whereas MuRF-1 and MAFbx mRNAs remained elevated.

As MG132 has been shown to increase skeletal muscle protein synthesis,[21] it could also prevent an increase in MuRF-1 and MAFbx expression by acting through the IGF-1/PI3K/Akt pathway, thereby increasing FoxO1 and FoxO3a phosphorylation states and keeping them in the cytosol. This hypothesis was not corroborated by our results, which showed no change in Akt or in FoxO1 and FoxO3a phosphorylation states.

The fact that HU did not increase UbCP level was unexpected, as several studies reported an increase with similar unloading time periods.[15,25] The explanation for this discrepancy is not obvious. Western blotting allows determination of the amount of ubiquitinated proteins but does not reflect a change in UbCP turnover. As a consequence, the ubiquitination–de-ubiquitination–degradation process might be increased even when the amount of UbCP remains stable. The fact that MuRF-1, MAFbx, and USP28 mRNA as well as β5 activity were all increased in response to HU supports this hypothesis.

In basal conditions β5 activity accounted for 79% of the total proteasome activity, whereas β1 and β2 accounted for 17% and 4%, respectively. These findings are in accordance with the proteasome relative catalytic activities reported previously in rat gastrocnemius.[26] In our experiment, absolute values for CTRL activities of β1, β2, and β5 subunits averaged 49.4 ± 2.3, 11.2 ± 0.8, and 229.5 ±

13.6 pmol AMC/min/mg protein, respectively. Proteasome β5 activity tended to increase with HU, whereas β1 and β2 activities did not change significantly. This is comparable to both absolute CTRL values and changes in catalytic activities observed in rat soleus muscle after 5-day HU.[25]

Protein extraction was performed in the presence of a protease inhibitor cocktail. One might expect that the use of protease inhibitors would lower proteasome activity. We tested the impact of the use of the protease inhibitor cocktail (Complete Mini; Roche Applied Science) during protein extraction on a proteasome β5 activity assay. Proteasome β5 activity was 39% lower when the protein extraction procedure was conducted in the absence of protease inhibitors ($n = 3$, $P = 0.002$). The protease inhibitor cocktail that we used is known to inhibit serine, cysteine, and aspartate proteases and metalloproteases, whereas the catalytic sites on the β1, β2, and β5 subunits of proteasome are threonine proteases.[27,28] Therefore, it is not surprising that β5 activity was not diminished. Instead, the inhibitor cocktail may prevent the degradation of proteasome subunits by serine, cysteine, and aspartate proteases and metalloproteases in the cells, thus leading to greater activity in vitro.

We did not observe any change in proteasome 20S α + β protein expression, suggesting that the increase in β5 activity with HU was due to a regulation of 20S affinity for its substrates or an increased intrinsic peptidase activity. This implicates the association of proteasome activator PA28 (i.e., 11S) or PA200 with the 20S proteasome.[29–31] In atrophy models, increased mRNA levels have been observed for both α and β PA28 subunits in response to unloading.[32] PA200 has been discovered more recently,[33] and its physiological function during disuse atrophy has not been established. Attachment of 19S to each extremity of 20S forms proteasome 26S, which is responsible for ubiquitin-mediated degradation. This process consumes adenosine triphosphate (ATP). As our in vitro assays were run in the absence of ATP, it is unlikely that the increase in β5 activity was due to 19S regulation. Posttranslational modifications, especially changes in phosphorylation states of 20S subunits, are other mechanisms that can influence 20S specific activity. Proteasome intrinsic activity can be increased by PKA phosphorylation of several 20S subunits.[34]

Although MG132 (1 mg/kg) injected every 48 h could diminish HU-induced atrophy, no significant proteasome inhibition was observed in HU+MG132 with in vitro assays when compared with HU. MG132 is known to affect mainly β5 activity,[35] and we were able to measure a strong inhibition of this activity in C2C12-cultured cells

incubated for 20 h with 10 μM MG132, thus suggesting that competitive inhibition of 20S by MG132 was maintained during the extraction procedure. It has been suggested that MG132 was less effective for inhibiting proteasome activity in skeletal muscle incubated in vitro than in cultured myogenic cells, likely because of a lower sensitivity of the differentiated muscle cell.[10] To the best of our knowledge, the pharmacokinetics of MG132 have not been studied systematically. The pharmacokinetics of other proteasome inhibitors have been determined, and blood concentrations of the drugs were measured by liquid chromatography with tandem mass spectrometry detection.[36,37] The drugs are rapidly removed from the vascular compartment. Alternative methods using proteasome in vitro activity measurement have been used to determine drug pharmacodynamic profiles.[38] Therefore, we analyzed the time-course of 20S proteasome inhibition by MG132 by measuring β5 activity in the gastrocnemius of NMRI mice injected intraperitoneally with 1 mg/kg MG132, which was the dose used in our study. The results show that the β5 proteasome was inhibited by 12% at 8 h after injection, and thereafter the activity was progressively restored. Due to the format of the data matrix (7 time-points and 3 animals for each time-point), application of a kinetic model was inappropriate, and our statistical analysis (ANOVA) did not reach the significance threshold. Although the main goal of our study was not to describe the pharmacodynamics of MG132, these data provide relevant information about the MG132-induced inhibition of proteasome β5 activity over time in skeletal muscle. Clearly, further studies are needed to describe the MG132 pharmacokinetics.

A limitation of this study is the absence of histological and functional analyses of the muscle. Having demonstrated that a proteasome inhibitor like MG132 is effective for protecting muscle mass after HU, further studies are required to shed light on structure, functional capabilities, and metabolic consequences of muscle mass preservation. This study included an early time-point of 6 days, and the potential beneficial effects of MG132 for longer periods as well as long-term tolerability still have to be assessed. Noticeably, HU+MG132 animals did not show any gross side effects when MG132 was given every other day. Although our results suggest an unexpected regulation of muscle-specific ligases as well as USP28 by MG132, other protein degradation pathways may be affected. Indeed, MG132 has been reported to inhibit cathepsins and calpains, but at a tenfold higher concentration.[8]

In conclusion, our results show that MG132 administration in vivo can repress muscle atrophy due to reduced muscle tension. Unexpectedly, this protective effect seems to involve regulation of expression of muscle ubiquitin-ligases. This observation reinforces the hypothesis that regulation of muscle ligases is critical for prevention of skeletal muscle atrophy. The signaling pathways responsible for this regulation still need to be fully elucidated.

REFERENCES

1. Lecker SH, Solomon V, Mitch WE, Goldberg AL. Muscle protein breakdown and the critical role of the ubiquitin–proteasome pathway in normal and disease states. J Nutr 1999;129(suppl):227S–237S.
2. Yimlamai T, Dodd SL, Borst SE, Park S. Clenbuterol induces muscle-specific attenuation of atrophy through effects on the ubiquitin–proteasome pathway. J Appl Physiol 2005;99:71–80.
3. Reid MB. Response of the ubiquitin–proteasome pathway to changes in muscle activity. Am J Physiol Regul Integr Comp Physiol 2005;288:R1423–R1431.
4. Taillandier D, Combaret L, Pouch MN, Samuels SE, Bechet D, Attaix D. The role of ubiquitin–proteasome-dependent proteolysis in the remodelling of skeletal muscle. Proc Nutr Soc 2004;63:357–361.
5. Bodine SC, Latres E, Baumhueter S, Lai VK, Nunez L, Clarke BA, et al. Identification of ubiquitin ligases required for skeletal muscle atrophy. Science 2001;294:1704–1708.
6. Baptista IL, Leal ML, Artioli GG, Aoki MS, Fiamoncini J, Turri AO, et al. Leucine attenuates skeletal muscle wasting via inhibition of ubiquitin ligases. Muscle Nerve 2010;41:800–808.
7. Dupont-Versteegden EE, Fluckey JD, Knox M, Gaddy D, Peterson CA. Effect of flywheel-based resistance exercise on processes contributing to muscle atrophy during unloading in adult rats. J Appl Physiol 2006;101:202–212.
8. Kisselev AF, Goldberg AL. Proteasome inhibitors: from research tools to drug candidates. Chem Biol 2001;8:739–758.
9. Combaret L, Adegoke OA, Bedard N, Baracos V, Attaix D, Wing SS. USP19 is a ubiquitin-specific protease regulated in rat skeletal muscle during catabolic states. Am J Physiol Endocrinol Metab 2005;288:E693–E700.
10. Tawa NE Jr, Odessey R, Goldberg AL. Inhibitors of the proteasome reduce the accelerated proteolysis in atrophying rat skeletal muscles. J Clin Invest 1997;100:197–203.
11. Kadlcikova J, Holecek M, Safranek R, Tilser I, Kessler BM. Effects of proteasome inhibitors MG132, ZL3VS and AdaAhx3L3VS on protein metabolism in septic rats. Int J Exp Pathol 2004;85:365–371.
12. Bonuccelli G, Sotgia F, Schubert W, Park DS, Frank PG, Woodman SE, et al. Proteasome inhibitor (MG-132) treatment of mdx mice rescues the expression and membrane localization of dystrophin and dystrophin-associated proteins. Am J Pathol 2003;163:1663–1675.
13. Safranek R, Ishibashi N, Oka Y, Ozasa H, Shirouzu K, Holecek M. Modulation of inflammatory response in sepsis by proteasome inhibition. Int J Exp Pathol 2006;87:369–372.
14. Supinski GS, Vanags J, Callahan LA. Effect of proteasome inhibitors on endotoxin-induced diaphragm dysfunction. Am J Physiol Lung Cell Mol Physiol 2009;296:L994–L1001.
15. Krawiec BJ, Frost RA, Vary TC, Jefferson LS, Lang CH. Hindlimb casting decreases muscle mass in part by proteasome-dependent proteolysis but independent of protein synthesis. Am J Physiol Endocrinol Metab 2005;289:E969–E980.
16. Beehler BC, Sleph PG, Benmassaoud L, Grover GJ. Reduction of skeletal muscle atrophy by a proteasome inhibitor in a rat model of denervation. Exp Biol Med (Maywood) 2006;231:335–341.
17. Deldicque L, Theisen D, Bertrand L, Hespel P, Hue L, Francaux M. Creatine enhances differentiation of myogenic C2C12 cells by activating both p38 and Akt/PKB pathways. Am J Physiol Cell Physiol 2007;293:C1263–1271.
18. Chopard A, Hillock S, Jasmin BJ. Molecular events and signalling pathways involved in skeletal muscle disuse-induced atrophy and the impact of countermeasures. J Cell Mol Med 2009;13:3032–3050.
19. Ferreira R, Vitorino R, Neuparth MJ, Appell HJ, Duarte JA, Amado F. Proteolysis activation and proteome alterations in murine skeletal

muscle submitted to 1 week of hindlimb suspension. Eur J Appl Physiol 2009;107:553–563.

20. Orlowski RZ, Stinchcombe TE, Mitchell BS, Shea TC, Baldwin AS, Stahl S, et al. Phase I trial of the proteasome inhibitor PS-341 in patients with refractory hematologic malignancies. J Clin Oncol 2002;20:4420–4427.

21. Holecek M, Muthny T, Kovarik M, Sispera L. Proteasome inhibitor MG-132 enhances whole-body protein turnover in rat. Biochem Biophys Res Commun 2006;345:38–42.

22. Koncarevic A, Jackman RW, Kandarian SC. The ubiquitin–protein ligase Nedd4 targets Notch1 in skeletal muscle and distinguishes the subset of atrophies caused by reduced muscle tension. FASEB J 2007;21:427–437.

23. Wing SS. Control of ubiquitination in skeletal muscle wasting. Int J Biochem Cell Biol 2005;37:2075–2087.

24. Zhang P, Chen X, Fan M. Signaling mechanisms involved in disuse muscle atrophy. Med Hypotheses 2007;69:310–321.

25. Berthon P, Duguez S, Favier FB, Amirouche A, Feasson L, Vico L, et al. Regulation of ubiquitin–proteasome system, caspase enzyme activities, and extracellular proteinases in rat soleus muscle in response to unloading. Pflugers Arch 2007;454:625–633.

26. Farout L, Lamare MC, Cardozo C, Harrisson M, Briand Y, Briand M. Distribution of proteasomes and of the five proteolytic activities in rat tissues. Arch Biochem Biophys 2000;374:207–212.

27. Glickman MH, Ciechanover A. The ubiquitin–proteasome proteolytic pathway: destruction for the sake of construction. Physiol Rev 2002; 82:373–428.

28. Lee DH, Goldberg AL. Proteasome inhibitors: valuable new tools for cell biologists. Trends Cell Biol 1998;8:397–403.

29. Ferrington DA, Husom AD, Thompson LV. Altered proteasome structure, function, and oxidation in aged muscle. FASEB J 2005;19: 644–646.

30. Stohwasser R, Salzmann U, Giesebrecht J, Kloetzel PM, Holzhutter HG. Kinetic evidences for facilitation of peptide channelling by the proteasome activator PA28. Eur J Biochem 2000;267:6221–6230.

31. Rechsteiner M, Hill CP. Mobilizing the proteolytic machine: cell biological roles of proteasome activators and inhibitors. Trends Cell Biol 2005;15:27–33.

32. Attaix D, Taillandier D, Combaret L, Ralliere C, Larbaud D, Aurousseau E, et al. Expression of subunits of the 19S complex and of the PA28 activator in rat skeletal muscle. Mol Biol Rep 1997;24:95–98.

33. Ustrell V, Pratt G, Gorbea C, Rechsteiner M. Purification and assay of proteasome activator PA200. Methods Enzymol 2005;398:321–329.

34. Zong C, Gomes AV, Drews O, Li X, Young GW, Berhane B, et al. Regulation of murine cardiac 20S proteasomes: role of associating partners. Circ Res 2006;99:372–380.

35. Myung J, Kim KB, Crews CM. The ubiquitin–proteasome pathway and proteasome inhibitors. Med Res Rev 2001;21:245–273.

36. Kupperman E, Lee EC, Cao Y, Bannerman B, Fitzgerald M, Berger A, et al. Evaluation of the proteasome inhibitor MLN9708 in preclinical models of human cancer. Cancer Res 2010;70:3853.

37. Attar EC, De Angelo DJ, Supko JG, D'Amato F, Zahrieh D, Sirulnik A, et al. Phase I and pharmacokinetic study of bortezomib in combination with idarubicin and cytarabine in patients with acute myelogenous leukemia. Clin Cancer Res 2008;14:1446–1454.

38. Lightcap ES, McCormack TA, Pien CS, Chau V, Adams J, Elliott PJ. Proteasome inhibition measurements: clinical application. Clin Chem 2000;46:673–683.